

## Far-Infrared Optical Properties of KCl and KBr†

K. W. JOHNSON\* AND E. E. BELL

*Department of Physics, The Ohio State University, Columbus, Ohio 43210*

(Received 17 February 1969; revised manuscript received 27 May 1969)

The far-infrared optical properties of KCl and KBr have been measured at  $T=300^\circ\text{K}$  by the method of asymmetric Fourier-transform spectroscopy. This method allows the simultaneous measurement of the amplitude and phase shifts of the radiation reflected or transmitted by the crystals. From reflectance data, the real and imaginary parts of the complex index of refraction were obtained in the spectral region from approximately 40 to  $360\text{ cm}^{-1}$ . Detailed numerical calculations for KCl were performed by employing a model in which the radiation was assumed to interact with the  $\mathbf{k}=0$  TO phonon mode via the first-order dipole moment and the subsequent decay of this mode by two-phonon processes. The frequency-dependent Hermitian and anti-Hermitian parts of the  $\mathbf{k}=0$  self-energy, arising from the cubic-lattice anharmonicity, were calculated by using the phonon frequencies and eigenvectors obtained from the Karo-Hardy deformation-dipole model. The complex index of refraction of KCl was calculated from the self-energy and the results are in reasonable agreement with experiment. Finally, a comparison is then made for KBr between the calculations performed by Cowley and our experimental data.

### I. INTRODUCTION

DURING the last decade, there has been considerable theoretical and experimental interest in examining the infrared lattice absorption in polar crystals. In diatomic crystals, such as KCl and KBr, the fundamental lattice-vibration absorption peak, at room temperature, is rather broad and exhibits sideband structure due to multiple-phonon interactions. The purpose of this paper is to investigate experimentally the optical properties of these two crystals in the spectral regions neighboring their fundamental absorption peaks and to compare the results with detailed numerical calculations.

The real and imaginary parts of the complex index of refraction have been measured at room temperature by the relatively new technique of asymmetric Fourier-transform spectroscopy.<sup>1,2</sup> One of the salient features of this method is that both the real and imaginary parts of the index of refraction can be measured directly in a single experiment. This is in contrast to standard techniques, where a spectrometer is used to measure, say, the reflectivity spectrum and then a Kramers-Kronig dispersion analysis is employed to obtain the phase spectrum.<sup>3</sup> The difficulty with the Kramers-Kronig procedure is that the alkali halides have a very low reflectance in the spectral region of interest, which leads to an inaccurately calculated phase. The asymmetric Fourier-transform method avoids this difficulty and, as will be discussed in Sec. II, is capable of yielding quantitative and qualitative information about the shape and sideband structure of the fundamental absorption peak.

In Sec. III, detailed numerical calculations are carried out for KCl, at  $T=300^\circ\text{K}$ , which utilize the phonon frequencies and eigenvectors provided by the deformation-dipole model employed by Karo and Hardy.<sup>4</sup> The calculations are based on a theoretical expression for the dielectric constant which includes the contributions from the linear dipole moment and the lattice anharmonicity. First, the frequency-dependent Hermitian and anti-Hermitian parts of the self-energy matrix, for the  $\mathbf{k}=0$  wave vector, were evaluated by summing the contributions arising from the cubic-lattice anharmonicity for 1000 evenly distributed wave vectors lying in the first Brillouin zone. The real and imaginary parts of the dielectric constant were then computed from the  $\mathbf{k}=0$  self-energy matrix in the spectral range from 40 to  $300\text{ cm}^{-1}$ .

Finally, the complex index of refraction of KCl was evaluated from the dielectric constant in this spectral region to permit comparisons to be made between the numerical calculations and experimental results. Such comparisons show that the secondary phonon structure present in the imaginary part of the index of refraction appears to be reasonably well accounted for, especially on the high-frequency side of the fundamental lattice absorption peak. The experimental data on the real part of the index of refraction show some structure between 180 and  $240\text{ cm}^{-1}$  that is qualitatively reproduced by the calculations although the quantitative agreement is only fair.

Cowley<sup>5</sup> has performed calculations on the optical properties of KBr and NaI at several temperatures. His work was based on the phonon frequencies and eigenvectors provided by the shell model of Woods *et al.*,<sup>6</sup> and he included the contributions to the dielectric constant from the second-order dipole moment in addition to the first-order moment. Cowley did not have detailed experimental data with which to compare his

† Work partially supported by the U. S. Air Force Cambridge Research Laboratories and the National Science Foundation.

\* Present address: Bell Telephone Laboratories, Holmdel, N. J. 07733.

<sup>1</sup> E. E. Bell, *Infrared Phys.* **6**, 57 (1966); E. E. Russell and E. E. Bell, *ibid.* **6**, 75 (1966).

<sup>2</sup> J. E. Chamberlain, J. E. Gibbs, and H. A. Gebbie, *Nature* **198**, 874 (1963); J. E. Chamberlain, F. D. Findlay, and H. A. Gebbie, *Appl. Opt.* **4**, 1382 (1965).

<sup>3</sup> A. Hadni, J. Claudel, D. Chanal, P. Strimer, and P. Vergnat, *Phys. Rev.* **163**, 836 (1967).

<sup>4</sup> A. M. Karo and J. R. Hardy, *Phys. Rev.* **129**, 2024 (1963).

<sup>5</sup> R. A. Cowley, *Advan. Phys.* **12**, 421 (1963).

<sup>6</sup> A. D. B. Woods, B. N. Brockhouse, R. A. Cowley, and W. Cochran, *Phys. Rev.* **131**, 1025 (1963).

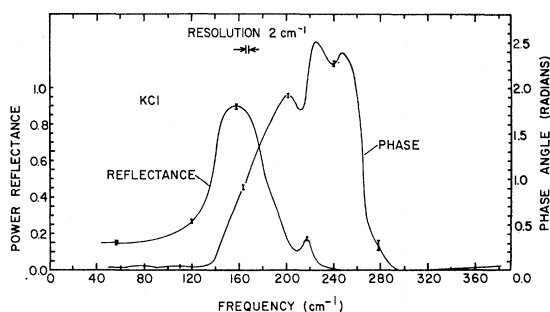


FIG. 1. Experimentally measured power reflectance  $R(\Omega)$  and phase spectrum  $\phi_r(\Omega)$  for KCl.

results and, therefore, in Sec. IV such a comparison is made for KBr using our experimental results.

## II. EXPERIMENTAL

Alkali halides are very strong absorbers of infrared radiation neighboring their lattice eigenfrequency. In order to obtain the optical constants of these materials by transmission measurements extremely thin ( $< 100 \mu$ ) samples are required whose surfaces are parallel and well polished.<sup>1</sup> Such samples have proved difficult to prepare, and therefore all of our measurements were obtained from single surface reflection. The complex amplitude reflectance can be expressed in polar form as

$$\hat{r}(\Omega) = r(\Omega)e^{i\phi_r(\Omega)}, \quad (1)$$

where  $\Omega$  is the frequency,  $r(\Omega)$  is the amplitude reflectance, and  $\phi_r(\Omega)$  is the phase shift of the reflected radiation. The caret indicates that the quantity beneath it is complex. The power reflectance  $R(\Omega)$  of the sample is given simply by  $R(\Omega) = r^2(\Omega)$ . Bell<sup>1</sup> has shown that asymmetric Fourier-transform spectroscopy is capable of simultaneously measuring both the amplitude and phase over the entire spectral region of interest.

Figures 1 and 2 show the experimentally measured power reflectance  $R(\Omega)$  and phase  $\phi_r(\Omega)$  for KCl and KBr, respectively. Figure 3 shows the power reflectance for KCl and KBr on an expanded vertical scale in the spectral region where the reflectance is less than 3%. The data for the reflectance and phase represent an average of at least four separate experimental runs. The vertical error bars that are drawn at various frequencies

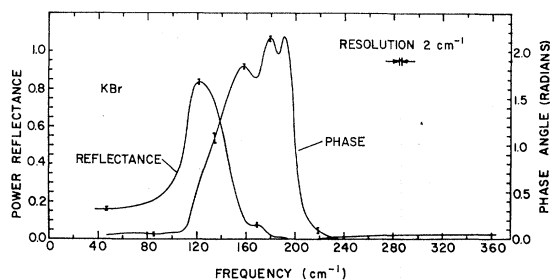


FIG. 2. Experimentally measured power reflectance  $R(\Omega)$  and phase spectrum  $\phi_r(\Omega)$  for KBr.

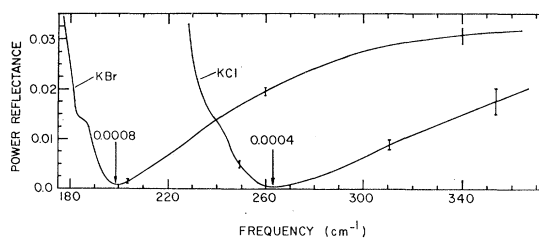


FIG. 3. Experimentally measured power reflectance for KCl and KBr in the spectral region where the reflectance is less than 3%.

on the curves shown in Figs. 1–3 represent the range of the peak-to-peak reproducibility of the data from the individual runs. It can be seen that the range of reproducibility is not constant but varies in different spectral regions.

Because the experimental results are to be compared with theoretical calculations, it is more convenient to express the optical properties in terms of the real and imaginary parts of the complex index of refraction  $\hat{N}(\Omega) = N(\Omega) + iK(\Omega)$  rather than the amplitude reflectance and phase.<sup>1</sup> Here  $N(\Omega)$  is the ordinary index of refraction, and  $K(\Omega)$  is called the extinction coefficient. Using the values for the power reflectance and phase, as shown in Figs. 1 and 2, the index of refraction and extinction coefficients for KCl and KBr were calculated and the results are shown in Figs. 4 and 5.

It should be mentioned that the values of the extinction coefficients  $K(\Omega)$  below  $120 \text{ cm}^{-1}$  for KCl and  $100 \text{ cm}^{-1}$  for KBr are not as accurate as those in the remaining spectral region. In this region the phase  $\phi_r(\Omega)$  becomes very small and it is difficult to measure accurately by the reflection technique. The uncertainty in the measurement of the phase  $\Delta\phi_r$  is given by the height of the vertical error bars shown in Figs. 1 and 2. At  $80 \text{ cm}^{-1}$ , for example,  $\Delta\phi_r/\phi_r \approx 0.3$  for both KCl and KBr, and it is easy to show that  $\Delta K/K \approx 0.3$ , where  $\Delta K$  is the uncertainty produced in the value of  $K$  due to the uncertainty in the measured value of the phase. In the spectral region where the phase is small, a more accurate determination of the extinction coefficient can be obtained if the measurements are made in transmission

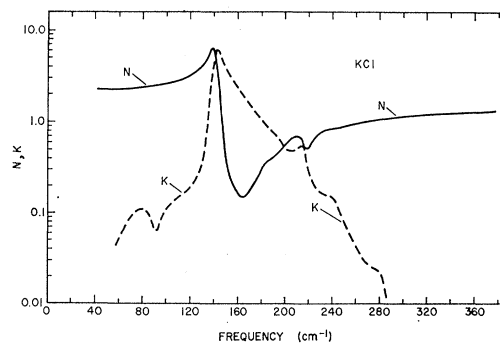


FIG. 4. Index of refraction  $N(\Omega)$  and extinction coefficient  $K(\Omega)$  for KCl.

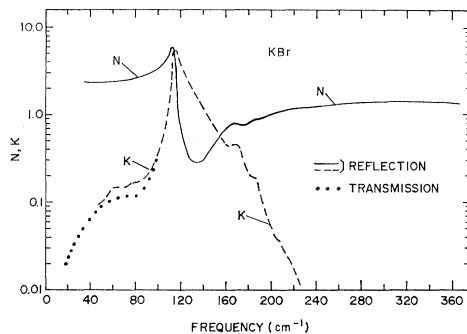


FIG. 5. Index of refraction  $N(\Omega)$  and extinction coefficient  $K(\Omega)$  for KBr.

rather than by reflection. Berg and Bell<sup>7</sup> have made some preliminary transmission measurements on thin (approximately  $115 \mu$ ) crystals of KBr. Because of the strong absorption that occurs around  $120 \text{ cm}^{-1}$ , their results are limited to the two spectral regions of  $30$  to  $105 \text{ cm}^{-1}$  and  $180$  to  $270 \text{ cm}^{-1}$ . Their values of  $K$  in the latter region agree quite well with our values. However, in the lower-frequency region their results indicate that our values for  $K$  are some 20% too high as shown in Fig. 5.

An examination of Fig. 3 shows that extremely small values of the power reflectance can be measured. The reason for this is that it is the amplitude reflectance  $r$ , rather than the power reflectance  $R$ , which is experimentally measured. For example, values of  $r$  as small as  $0.02$  can be measured to within an accuracy of  $0.005$ . This means that the power reflectance is  $0.0004$  with an accuracy of  $0.0002$ .

One final word is in order concerning the value of making direct experimental measurements of both the phase and amplitude reflectance. It is well known that, in principle, the phase spectrum can be obtained from a knowledge of the power reflectance by using the Kramers-Kronig relations. However, in practice, it is questionable whether the structure present on the phase curves could be discerned by using these relations if the power reflectance was measured in the conventional manner by using, for example, a spectrometer. An examination of Figs. 1-3 shows that the phase spectrum has significant structure due to phonon interactions in the region where the power reflectance becomes less than  $0.05$  ( $225$  to  $285 \text{ cm}^{-1}$  for KCl and  $170$  to  $220 \text{ cm}^{-1}$  for KBr). Values of the power reflectance as small as  $0.0004$  must be carefully measured if the Kramers-Kronig relations are to yield meaningful results, and spectrometers are not capable of making such measurements.

The power reflectances of these crystals have been previously measured by Mitsuishi *et al.*<sup>8</sup> Using a grating spectrometer, their results are generally compatible

<sup>7</sup> J. Berg and E. Bell (private communication).

<sup>8</sup> A. Mitsuishi, Y. Yamada, and H. Yoshinaga, *J. Opt. Soc. Am.* **52**, 14 (1962).

with the present ones. Our measurements indicate that the maximum values of the power reflectance tend to be slightly higher ( $0.9$  versus  $0.88$  for KCl and  $0.84$  versus  $0.8$  for KBr), and the shoulders occurring at  $185 \text{ cm}^{-1}$  for KBr and  $240 \text{ cm}^{-1}$  for KCl (see Fig. 3) cannot be seen in their data.

### III. THEORETICAL

#### A. Numerical Calculations

Our calculations on the far-infrared optical properties of KCl are based on an expression for the dielectric susceptibility that has been derived by Wallis and Maradudin,<sup>9</sup> and by Cowley.<sup>5</sup> This calculation uses only the first-order dipole moment and includes the contributions from the third-order anharmonicity coordinates. For crystals possessing cubic symmetry, the dielectric susceptibility tensor  $\chi_{\alpha\beta}$  is diagonal in the  $\alpha$  and  $\beta$  indices, and we shall adopt the notation that  $\chi_{\alpha\beta} = \chi_{\alpha\beta} \delta_{\alpha\beta} \equiv \chi_{\alpha}$ , where  $\delta_{\alpha\beta}$  is the usual Kronecker  $\delta$ . The susceptibility, as a function of the frequency  $\Omega$ , is given by

$$\chi_{\alpha}(\Omega) = \chi_{\alpha}^E + \frac{1}{Nv\hbar} \sum_j \frac{2\omega(0j)M_{\alpha}^2(0j)}{\omega^2(0j) - \Omega^2 + 2\omega(0j)[\Delta(0j; \Omega) - i\Gamma(0j; \Omega)]}. \quad (2)$$

In this expression  $\chi_{\alpha}^E$  is the electronic contribution to the susceptibility,  $v$  is the volume of the KCl unit cell,  $N$  is the number of unit cells in the crystal, and  $\omega(0j)$  is the angular frequency of the phonon mode, in the harmonic approximation, belonging to the wave vector  $\mathbf{k}=0$  and branch index  $j$ .  $M_{\alpha}(0j)$  is the  $\alpha$  component of the coefficient of the leading term in the expansion of the crystal dipole moment operator in powers of the phonon field operators.<sup>5</sup>  $\Delta(0j; \Omega)$  and  $\Gamma(0j; \Omega)$  are the frequency-dependent Hermitian and anti-Hermitian parts of the proper self-energy matrix, which arise from the anharmonicity of the lattice, for the  $\mathbf{k}=0$  mode belonging to the phonon branch  $j$ . Ipatova *et al.*<sup>9</sup> have shown that the coefficient  $M_{\alpha}(0j)$  is nonvanishing only if the branch index  $j$  refers to any one of the two TO branches. Therefore, the summation appearing in Eq. (2) is only over the two TO branches. Contributions to  $\chi_{\alpha}(\Omega)$  arising from the second-order dipole moment have been worked out by Cowley,<sup>5</sup> although they are not included in our calculations because we have assumed that they are less important than that due to anharmonicity alone.<sup>10</sup>

The lowest-order expressions for  $\Delta(0j; \Omega)$  and  $\Gamma(0j; \Omega)$ , which arise from the thermal expansion and anharmonicity of the lattice, have been derived by

<sup>9</sup> R. F. Wallis and A. A. Maradudin, *Phys. Rev.* **125**, 1277 (1962); I. P. Ipatova, A. A. Maradudin, and R. F. Wallis, *Fiz. Tverd. Tela* **8**, 1064 (1966) [English transl.: *Soviet Phys.—Solid State* **8**, 850 (1966)].

<sup>10</sup> P. N. Keating and G. Rupprecht, *Phys. Rev.* **138**, 866 (1965).

Cowley<sup>5,11</sup> and by Maradudin and Fein.<sup>12</sup> The Hermitian part of the  $\mathbf{k}=0$  self-energy  $\Delta(0j; \Omega)$  is given by a sum of three terms

$$\Delta(0j; \Omega) = \Delta_1(0j) + \Delta_2(0j) + \Delta_3(0j; \Omega), \quad (3)$$

where  $\Delta_1(0j)$  and  $\Delta_2(0j)$  are frequency-independent terms that arise from the thermal expansion of the crystal and the fourth-order anharmonicity of the lattice potential.  $\Delta_3(0j; \Omega)$  is frequency-dependent and is written as<sup>5</sup>

$$\Delta_3(0j; \Omega) = \frac{-18}{\hbar^2} \sum_{\mathbf{k}_1 j_1} \sum_{\mathbf{k}_2 j_2} |V^{(3)}(0j; \mathbf{k}_1 j_1; \mathbf{k}_2 j_2)|^2 R(\Omega), \quad (4)$$

where

$$R(\Omega) = [n(\mathbf{k}_1 j_1) + n(\mathbf{k}_2 j_2) + 1] \times \{ [\omega(\mathbf{k}_1 j_1) + \omega(\mathbf{k}_2 j_2) + \Omega]_P^{-1} + [\omega(\mathbf{k}_1 j_1) + \omega(\mathbf{k}_2 j_2) - \Omega]_P^{-1} + [n(\mathbf{k}_2 j_2) - n(\mathbf{k}_1 j_1)] \{ [\omega(\mathbf{k}_1 j_1) - \omega(\mathbf{k}_2 j_2) - \Omega]_P^{-1} - [-\omega(\mathbf{k}_1 j_1) + \omega(\mathbf{k}_2 j_2) - \Omega]_P^{-1} \}. \quad (5)$$

Each of the two summations appearing in Eq. (4) extends over all of the phonon modes of the crystal, where  $\mathbf{k}$  is the wave vector of the mode and  $j$  is the branch index.  $V^{(3)}(0j; \mathbf{k}_1 j_1; \mathbf{k}_2 j_2)$  is the cubic-coupling coefficient that connects the three modes  $(0j)$ ,  $(\mathbf{k}_1 j_1)$ , and  $(\mathbf{k}_2 j_2)$  via the cubic anharmonicity of the lattice. An explicit expression for  $V^{(3)}$  that is used in our calculations is given later in this section.  $n(\mathbf{k}j)$  is the occupation number for the mode  $(\mathbf{k}j)$  and it is given by

$$n(\mathbf{k}j) = [\exp(\hbar\omega(\mathbf{k}j)/k_B T) - 1]^{-1}, \quad (6)$$

where  $\omega(\mathbf{k}j)$  is the frequency of the mode in the harmonic approximation,  $T$  is the temperature, and  $k_B$  is

Boltzmann's constant. The notation  $1/[X]_P$  means that the principal part of the expression is to be used, and hence the  $X=0$  contributions to the summations appearing in Eqs. (4) and (5) are excluded. Expressions for  $\Delta_1(0j)$  and  $\Delta_2(0j)$  have not been written because, being independent of frequency, they contribute only a constant term to  $\Delta(0j; \Omega)$ . In Sec. III D it is shown that if  $\Delta(0j; \Omega) \ll \omega(0j)$ , where  $\omega(0j)$  is the  $\mathbf{k}=0$  TO phonon frequency, one can work within the approximation that

$$\Delta(0j; \Omega) \approx \Delta_3(0j; \Omega), \quad (7)$$

which obviates calculating  $\Delta_1$  and  $\Delta_2$ .

The anti-Hermitian part of the  $\mathbf{k}=0$  self-energy is<sup>5</sup>

$$\Gamma(0j; \Omega) = \frac{18\pi}{\hbar^2} \sum_{\mathbf{k}_1 j_1} \sum_{\mathbf{k}_2 j_2} |V^{(3)}(0j; \mathbf{k}_1 j_1; \mathbf{k}_2 j_2)|^2 S(\Omega), \quad (8)$$

where

$$S(\Omega) = -[n(\mathbf{k}_1 j_1) + n(\mathbf{k}_2 j_2) + 1] \times \{ \delta[\omega(\mathbf{k}_1 j_1) + \omega(\mathbf{k}_2 j_2) + \Omega] - \delta[-\omega(\mathbf{k}_1 j_1) - \omega(\mathbf{k}_2 j_2) + \Omega] - [n(\mathbf{k}_1 j_1) - n(\mathbf{k}_2 j_2)] \{ \delta[\omega(\mathbf{k}_2 j_2) - \omega(\mathbf{k}_1 j_1) + \Omega] - \delta[\omega(\mathbf{k}_1 j_1) - \omega(\mathbf{k}_2 j_2) + \Omega] \}. \quad (9)$$

The notation appearing in Eqs. (8) and (9) is the same as that used in Eqs. (4)–(6), except that  $\delta(X)$  represents a Dirac  $\delta$  function. The format for calculating  $\chi_a(\Omega)$  was to first evaluate  $\Delta(0j; \Omega)$  and  $\Gamma(0j; \Omega)$  over a broad spectral region (approximately 0–300  $\text{cm}^{-1}$ ) and then substitute these functions into Eq. (2) to determine the dielectric susceptibility.

The cubic-coupling coefficient that appears in Eqs. (4) and (8) is given explicitly by<sup>13</sup>

$$V^{(3)}(0j; \mathbf{k}_1 j_1; \mathbf{k}_2 j_2) = \frac{1}{6N^{3/2}} \left( \frac{\hbar^3}{8\omega(0j)\omega(\mathbf{k}_1 j_1)\omega(\mathbf{k}_2 j_2)} \right)^{1/2} \Delta(\mathbf{k}_1 + \mathbf{k}_2) \left[ \frac{1}{2} \sum_{LK} \sum_{L'K'} \sum_{\alpha\beta\gamma} \phi_{\alpha\beta\gamma}(LK; L'K') \left( \frac{m_\alpha(0j|K)}{M_K^{1/2}} - \frac{m_\alpha(0j|K')}{M_{K'}^{1/2}} \right) \times \left( \frac{m_\beta(\mathbf{k}_1 j_1|K)}{M_K^{1/2}} \exp(2\pi i \mathbf{k}_1 \cdot [\mathbf{X}(L) + \mathbf{X}(K)]) - \frac{m_\beta(\mathbf{k}_1 j_1|K')}{M_{K'}^{1/2}} \exp(2\pi i \mathbf{k}_1 \cdot [\mathbf{X}(L') + \mathbf{X}(K')]) \right) \times \left( \frac{m_\gamma(\mathbf{k}_2 j_2|K)}{M_K^{1/2}} \exp(2\pi i \mathbf{k}_2 \cdot [\mathbf{X}(L) + \mathbf{X}(K)]) - \frac{m_\gamma(\mathbf{k}_2 j_2|K')}{M_{K'}^{1/2}} \exp(2\pi i \mathbf{k}_2 \cdot [\mathbf{X}(L') + \mathbf{X}(K')]) \right) \right]. \quad (10)$$

In this expression  $\mathbf{X}(L)$  is a vector from an arbitrary origin in the lattice to the  $L$ th unit cell and  $\mathbf{X}(K)$  is a vector from the origin of the  $L$ th cell to the equilibrium position of the  $K$ th atom located within that cell. The double summation  $\sum_{LK}$  means that  $L$  sums over the  $N$  unit cells in the crystal and  $K$  ranges over the two

atoms in the unit cell. The prime appearing in Eq. (10) on the summation symbol  $\sum'$  means that the terms in which  $L'K' = LK$  are to be excluded from the summation.  $M_K$  is the mass of the  $K$ th kind of atom,  $\omega(\mathbf{k}j)$  is the frequency of the normal mode described by the wave vector  $\mathbf{k}$  and branch index  $j$ , and  $m_\alpha(\mathbf{k}j|K)$  is the  $\alpha$ th component of the eigenvector belonging to this mode. This eigenvector is the one defined by Karo,<sup>14</sup>

<sup>11</sup> R. A. Cowley, in *Phonons: In Perfect Lattices and in Lattices with Point Imperfections* edited by R. W. H. Stevenson (Plenum Press, Inc., New York, 1966).

<sup>12</sup> A. A. Maradudin and A. E. Fein, *Phys. Rev.* **128**, 2589 (1962).

<sup>13</sup> A. A. Maradudin, P. A. Flinn, and R. A. Coldwell-Horsfall, *Ann. Phys. (N. Y.)* **15**, 337 (1961), especially p. 340.

<sup>14</sup> A. M. Karo, *J. Chem. Phys.* **31**, 1489 (1959).

TABLE I. Quantities used in the calculation of the complex index of refraction of KCl at room temperature.

Lattice constant <sup>a</sup>	$r_0$	$3.139 \times 10^{-8}$ cm
Compressibility <sup>a</sup>	$\beta$	$5.63 \times 10^{-12}$ cm <sup>2</sup> /dyn
Electron charge	$e$	$4.8 \times 10^{-10}$ esu
Madelung constant	$\alpha$	1.7476
Parameters of the potential function	$\rho$ $C$	$0.324 \times 10^{-8}$ cm $3.60 \times 10^{-9}$ erg
First, second, and third derivatives of the potential function	$\phi'(r_0)$ $\phi''(r_0)$ $\phi'''(r_0)$	$-6.25 \times 10^{-5}$ erg/cm $+1.93 \times 10^4$ erg/cm <sup>2</sup> $-5.96 \times 10^{12}$ erg/cm <sup>3</sup>
Mass of the K <sup>+</sup> ion	$M_0$	$64.916 \times 10^{-24}$ g
Mass of the Cl <sup>-</sup> ion	$M_1$	$58.867 \times 10^{-24}$ g
$\frac{m_x(0j 0)}{M_0^{1/2}} - \frac{m_x(0j 1)}{M_1^{1/2}}$		$0.18 \times 10^{12}$ g <sup>-1/2</sup>
Volume of the KCl unit cell	$v$	$6.192 \times 10^{-23}$ cm <sup>3</sup>
Ionic polarizabilities <sup>a</sup>	$\alpha_+$ $\alpha_-$	$1.201 \times 10^{-24}$ cm <sup>3</sup> $2.974 \times 10^{-24}$ cm <sup>3</sup>
"Effective charge" <sup>a</sup>	$ e^* $	$3.84 \times 10^{-10}$ esu
Coefficients of the linear dipole moment operator	$\epsilon$ $M_x(0j)$	$5.35 \times 10^{-10}$ esu $96.31 [N\hbar/2\omega(0j)]^{+1/2}$
Electronic susceptibility	$\chi_\alpha^E$	0.094

\* See Ref. 4.

and it is related to the eigenvector used by Born and Huang<sup>15</sup>  $e_\alpha(\mathbf{k}j|K)$  by

$$m_\alpha(\mathbf{k}j|K) = e_\alpha(\mathbf{k}j|K) e^{2\pi i \mathbf{k} \cdot \mathbf{X}(K)}. \quad (11)$$

The  $\Delta$  function in Eq. (10) shows the conservation of crystal momentum, and it has the property that

$$\Delta(\mathbf{k}_1 + \mathbf{k}_2) = 1 \quad \text{if } \mathbf{k}_1 + \mathbf{k}_2 = \mathbf{0} \text{ or } \mathbf{G}, \text{ where } \mathbf{G} \text{ is a reciprocal-lattice vector} \\ = 0 \quad \text{otherwise.} \quad (12)$$

$\phi_{\alpha\beta\gamma}(LK; L'K')$  is the atomic force constant between two ions, the first one of which is located at  $\mathbf{X}(L) + \mathbf{X}(K)$  and the second one at  $\mathbf{X}(L') + \mathbf{X}(K')$ .  $\alpha$ ,  $\beta$ , and  $\gamma$  each extend over the three Cartesian components  $x$ ,  $y$ , and  $z$ . An explicit expression for  $\phi_{\alpha\beta\gamma}(LK; L'K')$  is given later in Eq. (17).

## B. Potential Function and Third-Order Force Constants

In order to evaluate the cubic-coupling coefficient  $V^{(3)}(0j; \mathbf{k}_1 j_1; \mathbf{k}_2 j_2)$  certain assumptions must be made about the nature of the forces that interact between the ions in the lattice. In our calculations we have chosen a potential function which is of the form<sup>5</sup>

$$\phi(r) = +C e^{-r/\rho}, \quad (13)$$

where  $\phi(r)$  is the potential energy between a pair of ions separated by a distance  $r$ . Equation (13) represents the short-range central-force repulsive potential which

results from the overlap of two neighboring ions; the Coulomb contribution to  $\phi(r)$  has not been included because the overlap term dominates the anharmonic effects.  $C$  and  $\rho$  are parameters that can be evaluated, for a given temperature, by relating the first derivative  $\phi'(r)$  and the second derivative  $\phi''(r)$  of the potential function  $\phi(r)$  to the experimentally observed values of the lattice constant  $r_0$  and the compressibility  $\beta$ .<sup>16</sup>  $C$  and  $\rho$  are evaluated by the relations

$$\rho = (\alpha e^2 / 2r_0^2) (9r_0 / \beta + \alpha e^2 / r_0^3)^{-1} \quad (14)$$

and

$$C = (\alpha \rho e^2 / 6r_0^2) e^{+r_0/\rho}. \quad (15)$$

The values of the constants used in the lattice calculations are given in Table I together with the derived values of  $\rho$ ,  $C$ ,  $\phi''(r_0)$ , and  $\phi'''(r_0)$ .

The third-order force constants  $\phi_{\alpha\beta\gamma}(LK; L'K')$  that appear in Eq. (10) depend only on the equilibrium distance  $r_0$  between the ions ( $LK$ ) and ( $L'K'$ ).  $\phi_{\alpha\beta\gamma}(r_0)$  is defined as

$$\phi_{\alpha\beta\gamma}(r_0) \equiv \left. \frac{\partial^3 \phi(r)}{\partial r_\alpha \partial r_\beta \partial r_\gamma} \right|_{r=r_0}, \quad (16)$$

where  $r_\alpha$  is the  $\alpha$ th Cartesian component of the distance between two ions. It is straightforward to evaluate Eq. (16) with the result that

$$\phi_{\alpha\beta\gamma}(r_0) = \left[ \frac{r_\alpha r_\beta r_\gamma}{r^3} \left( \phi'''(r) - \frac{3}{r} \phi''(r) + \frac{3}{r^2} \phi'(r) \right) \right. \\ \left. + (\delta_{\alpha\beta} r_\gamma + \delta_{\beta\gamma} r_\alpha + \delta_{\gamma\alpha} r_\beta) \right. \\ \left. \times \frac{[\phi''(r) - (1/r)\phi'(r)]}{r^2} \right] \Big|_{r=r_0}, \quad (17)$$

where  $\delta_{\alpha\beta}$  is the usual Kronecker  $\delta$ . We shall also neglect the  $\phi'(r)$  terms in (17) because they are small compared with the second- and third-derivative terms.

## C. Evaluation of Cubic-Coupling Coefficient

$$V^{(3)}(0j; \mathbf{k}_1 j_1; \mathbf{k}_2 j_2)$$

The general expression for  $V^{(3)}(0j; \mathbf{k}_1 j_1; \mathbf{k}_2 j_2)$  as given by Eq. (10) involves lattice summations of the form  $\sum_{LK} \sum_{L'K'}$  and a triple summation over the Cartesian components  $\sum_{\alpha\beta\gamma}$ . Because of the translational invariance of the lattice the sum over  $L$  is  $N$  times the contribution to  $V^{(3)}$  from one unit cell. For a fixed value of  $K$ ,  $\sum_{L'K'}$  was assumed to include only the contributions from the six nearest neighbors of  $K$ . The wave vector of the incident radiation was assumed to be parallel to a symmetry direction in the crystal and to have its transverse polarization in the  $+x$  direction. Therefore, the eigenvector of the  $\mathbf{k} = 0$  TO phonon mode has only  $x$  components  $m_x(0j|K)$ , while the  $y$  and  $z$  components are zero. Using the above-mentioned assumptions the summations appearing in Eq. (10) have

<sup>15</sup> M. Born and K. Huang, *Dynamical Theory of Crystal Lattices* (Oxford University Press, Oxford, 1954), p. 298.

<sup>16</sup> See Ref. 15, p. 24.

been carried out in a straightforward, but tedious, manner to yield

$$\begin{aligned}
 & V^{(3)}(0j; \mathbf{k}_1 j_1; \mathbf{G} - \mathbf{k}_1 j_2) \\
 &= \frac{i}{3N^{1/2}(M_0 M_1)^{1/2}} \left( \frac{m_x(0j|0)}{M_0^{1/2}} - \frac{m_x(0j|1)}{M_1^{1/2}} \right) \left( \frac{\hbar^3}{8\omega(0j)\omega(\mathbf{k}_1 j_1)\omega(\mathbf{G} - \mathbf{k}_1 j_2)} \right)^{1/2} \\
 & \times \left[ \left( \phi'''(r_0) [m_x(\mathbf{k}_1 j_1|0)m_x(\mathbf{G} - \mathbf{k}_1 j_2|1) \cos(2\pi r_0 \mathbf{G} \cdot \mathbf{e}_x) - m_x(\mathbf{k}_1 j_1|1)m_x(\mathbf{G} - \mathbf{k}_1 j_2|0)] \right. \right. \\
 & \left. \left. + \frac{\phi''(r_0)}{r_0} \sum_{\alpha=y,z} [m_\alpha(\mathbf{k}_1 j_1|0)m_\alpha(\mathbf{G} - \mathbf{k}_1 j_2|1) \cos(2\pi r_0 \mathbf{G} \cdot \mathbf{e}_\alpha) - m_\alpha(\mathbf{k}_1 j_1|1)m_\alpha(\mathbf{G} - \mathbf{k}_1 j_2|0)] \right) \sin(2\pi r_0 \mathbf{k}_1 \cdot \mathbf{e}_x) \right. \\
 & \left. + \frac{\phi''(r_0)}{r_0} \sum_{\delta=y,z} \left( [m_\delta(\mathbf{k}_1 j_1|0)m_\delta(\mathbf{G} - \mathbf{k}_1 j_2|1) \cos(2\pi r_0 \mathbf{G} \cdot \mathbf{e}_\delta) - m_\delta(\mathbf{k}_1 j_1|1)m_\delta(\mathbf{G} - \mathbf{k}_1 j_2|0)] \right. \right. \\
 & \left. \left. + m_x(\mathbf{k}_1 j_1|0)m_\delta(\mathbf{G} - \mathbf{k}_1 j_2|1) \cos(2\pi r_0 \mathbf{G} \cdot \mathbf{e}_\delta) - m_x(\mathbf{k}_1 j_1|1)m_\delta(\mathbf{G} - \mathbf{k}_1 j_2|0) \right) \sin(2\pi r_0 \mathbf{k}_2 \cdot \mathbf{e}_\delta) \right]. \quad (18)
 \end{aligned}$$

In Eq. (18),  $\mathbf{G}$  is a vector of the reciprocal lattice and  $\mathbf{e}_\delta$  is a unit vector pointing in the  $\delta$ th Cartesian direction in  $\mathbf{k}$  space. Maradudin *et al.*<sup>17</sup> have shown that the two components of the  $\mathbf{k} = 0$  eigenvector are so related that

$$\begin{aligned}
 \left( \frac{m_x(0j|0)}{M_0^{1/2}} - \frac{m_x(0j|1)}{M_1^{1/2}} \right) &= \left( \frac{M_0 + M_1}{M_0 M_1} \right)^{1/2} \\
 &= 0.18 \times 10^{+12} \text{ g}^{-1/2}, \quad (19)
 \end{aligned}$$

where  $M_0$  and  $M_1$  are the masses of the two ions in the unit cell and are given in Table I.

#### D. Renormalization

There is one important point that must be considered with regards to the frequencies and eigenvectors that are to be used in evaluating the susceptibility. The expressions for  $\Delta(0j; \Omega)$ ,  $\Gamma(0j; \Omega)$ , and the cubic-coupling coefficient  $V^{(3)}$  involve the phonon frequencies  $\omega(\mathbf{k}j)$  and their associated eigenvectors  $m_\alpha(\mathbf{k}j|K)$  of the *harmonic lattice*. However, as previously mentioned, our calculations were made by using the frequencies and eigenvectors which were obtained from the Karo-Hardy deformation-dipole model.<sup>18</sup> The frequencies obtained from this model are presumably the *actual* lattice frequencies (not the harmonic frequencies) which would be obtained, say, by performing an inelastic neutron scattering experiment. Therefore, the room-temperature frequencies given by the Karo-Hardy model already have the effects of the lattice anharmonicity and thermal expansion included in them and they are *per se* acceptable as the harmonic frequencies required for the calculation of  $\Delta(0j; \Omega)$ ,  $\Gamma(0j; \Omega)$ , and  $\chi(\Omega)$ .

<sup>17</sup> A. A. Maradudin, E. W. Montroll, and G. H. Weiss, *Theory of Lattice Dynamics in the Harmonic Approximation* (Academic Press Inc., New York, 1963), p. 14.

<sup>18</sup> The eigendata are tabulated in a report that was kindly sent to us by Dr. A. M. Karo, University of California, Lawrence Radiation Laboratory, Report No. UCRL-14822, 1966 (unpublished).

Cowley<sup>5</sup> has proposed a renormalization scheme such that the expressions for  $\Delta(0j; \Omega)$ ,  $\Gamma(0j; \Omega)$ , and  $\chi(\Omega)$  will involve the actual lattice frequencies and eigenvectors rather than the harmonic eigendata. He has shown that if  $\Gamma(0j; \Omega)$ , is small it is a reasonable approximation to renormalize the harmonic frequencies by replacing them with the so-called quasiharmonic frequencies  $\omega_Q(\mathbf{k}j)$ , which are given approximately by

$$\omega_Q(\mathbf{k}j) \approx \omega(\mathbf{k}j) + \Delta[\mathbf{k}j; \omega_Q(\mathbf{k}j)], \quad (20)$$

where  $\Delta[\mathbf{k}j; \omega_Q(\mathbf{k}j)]$  is the Hermitian part of the self-energy matrix evaluated at the quasiharmonic frequency  $\omega_Q(\mathbf{k}j)$ . The quasiharmonic frequencies given by Eq. (20) define the centers of the one-phonon neutron scattering groups<sup>19</sup> and, therefore, represent the actual lattice frequencies. However, the actual lattice frequencies are those given by the Karo-Hardy deformation-dipole model, and they are the quasiharmonic frequencies defined by Eq. (20). According to Cowley's renormalization program the real and imaginary parts of the self-energy matrix can be calculated by simply replacing the harmonic frequencies and eigenvectors by the Karo-Hardy eigendata. From Eqs. (2), (3), and (20) it can be seen that the susceptibility  $\chi_\alpha(\Omega)$  has a denominator of the form

Denominator

$$\begin{aligned}
 &= \omega_Q^2(0j) - \Omega^2 + 2\{\omega_Q(0j) - \Delta[0j; \omega_Q(0j)]\} \\
 & \times \{\Delta_\delta(0j; \Omega) - \Delta_\delta[0j; \omega_Q(0j)] - i\Gamma(0j; \Omega)\} \\
 & \quad - \Delta^2[0j; \omega_Q(0j)]. \quad (21)
 \end{aligned}$$

Equation (21) can be somewhat simplified by noting that  $\omega_Q(0j) \gg \Delta[0j; \omega_Q(0j)]$ . This approximation obviates calculating the frequency-independent terms  $\Delta_1$  and  $\Delta_2$  [see Eq. (3)].

<sup>19</sup> E. R. Cowley and R. A. Cowley, Proc. Roy. Soc. (London) **A287**, 259 (1965).

Using the above-mentioned approximations, the dielectric susceptibility can be written as

$$\chi_{\alpha}(\Omega) = \chi_{\alpha}^B + \frac{1}{Nv\hbar} \frac{2M_{\alpha}^2(0j)\omega_Q(0j)}{\omega_Q^2(0j) - \Omega^2 + 2\omega_Q(0j)\{\Delta_3(0j; \Omega) - \Delta_3[0j; \omega_Q(0j)] - i\Gamma(0j; \Omega)\}}, \quad (22)$$

where  $\Delta_3$ ,  $\Gamma$ , and  $M_{\alpha}(0j)$  are evaluated by using the Karo-Hardy frequencies and eigenvectors. The summation over the branch indices  $\sum_j$  has now been dropped in writing Eq. (22), because there is only one infrared-active optical mode. Equation (22) represents the form that the dielectric susceptibility takes in the quasi-harmonic approximation.

### E. Numerical Evaluation of $\Delta_3(0j; \Omega)$ , $\Gamma(0j; \Omega)$ , and the Complex Index of Refraction

The lattice frequencies and eigenvectors used in calculating  $\Delta_3$  and  $\Gamma$  were obtained for 1000 wave vectors that were evenly spaced throughout the first Brillouin zone. Since the KCl unit cell has six degrees of freedom, the eigendata represented a total of 6000 modes. Because of the symmetry possessed by the Brillouin zone, Karo and Hardy restricted the calculation of the eigendata to those wave vectors that laid within a 1/48 section of the zone (called the irreducible zone<sup>14</sup>) which contained exactly 48 wave vectors. The frequencies and eigenvectors belonging to wave vectors lying outside of the irreducible zone were obtained by applying the appropriate symmetry operations of the cubic lattice to the frequencies and eigenvectors belonging to the irreducible zone.<sup>20</sup>

The numerical computations involved in calculating  $\Delta_3$  and  $\Gamma$  were performed on an IBM 7094 computer. The representations for the principal part  $(1/X)_P$  and the  $\delta$  function  $\delta(X)$  appearing in Eqs. (5) and (9) were chosen to be<sup>12</sup>

$$\left(\frac{1}{X}\right)_P = \lim_{\epsilon \rightarrow 0^+} \frac{X}{X^2 + \epsilon^2} \quad (23)$$

and

$$\delta(X) = \lim_{\epsilon \rightarrow 0^+} \frac{1}{\pi} \frac{\epsilon}{X^2 + \epsilon^2}. \quad (24)$$

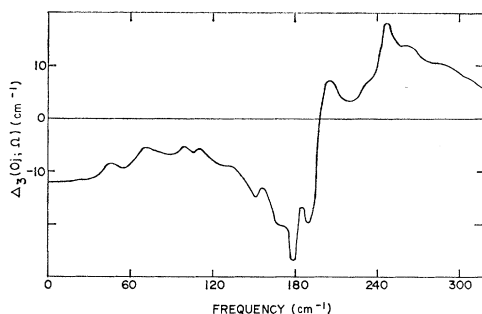


Fig. 6. Hermitian part of the  $\mathbf{k}=0$  self-energy matrix for KCl.

<sup>20</sup> J. Neuberger and R. D. Hatcher, J. Chem. Phys. **34**, 1733 (1961), especially p. 1739.

Theoretically, the value of  $\epsilon$  must be made infinitesimally small; however, in practice it should be made as small as possible to be consistent with the amount of eigendata available. For our calculations, a value of  $\epsilon = 1.5 \text{ cm}^{-1}$  was found to be satisfactory.

The procedure used in calculating  $\Delta_3(0j; \Omega)$  and  $\Gamma(0j; \Omega)$  was as follows: The computer selected an independent wave vector  $\mathbf{k}_1$  and the branch index  $j_1$ . The dependent wave vector  $\mathbf{k}_2$  with branch index  $j_2$  was then determined from Eq. (12) by  $\mathbf{k}_2 = \mathbf{G} - \mathbf{k}_1$ , where  $\mathbf{G}$  is a unique vector of the reciprocal lattice that ensures that  $\mathbf{k}_2$  lies in the first Brillouin zone. Having selected  $(\mathbf{k}_1 j_1)$  and  $(\mathbf{k}_2 j_2)$  the computer then evaluated  $V^{(3)}(0j; \mathbf{k}_1 j_1; \mathbf{k}_2 j_2)$  according to Eq. (18) with the factor  $N^{-1/2}$ , where  $N$  is the number of unit cells in the crystal, being left undetermined, since it is cancelled out when  $V^{(3)}$  is substituted into the expressions for  $\Delta_3$  and  $\Gamma$ . The computer then calculated the contributions to  $\Delta_3(0j; \Omega)$  and  $\Gamma(0j; \Omega)$  from the modes  $(\mathbf{k}_1 j_1)$  and  $(\mathbf{k}_2 j_2)$  as indicated in Eqs. (4), (5), (8), and (9). Both  $\Delta_3$  and  $\Gamma$  were evaluated at discrete frequencies  $\Omega_j$  which ranged from 0 to 380  $\text{cm}^{-1}$ , in steps of 0.3  $\text{cm}^{-1}$ . A new combination of the branch indices  $j_1$  and  $j_2$  was then selected (keeping  $\mathbf{k}_1$  and  $\mathbf{k}_2$  fixed) and the above procedure was repeated until all possible combinations were exhausted. Since  $j_1, j_2 = 1, \dots, 6$ , there are a total of 36 contributions to  $\Delta_3(0j; \Omega)$  and  $\Gamma(0j; \Omega)$  for a given value of the independent wave vector  $\mathbf{k}_1$ . A new independent wave vector was then chosen and the above-mentioned calculation was repeated until the contributions from all of the 1000 independent wave vectors in the first Brillouin zone had been summed. The results of these calculations for  $\Delta_3(0j; \Omega)$  and  $\Gamma(0j; \Omega)$  are shown in Figs. 6 and 7, respectively, where smooth curves have been drawn through the discrete calculated data.

Having calculated  $\Delta_3(0j; \Omega)$  and  $\Gamma(0j; \Omega)$ , it is straightforward to calculate the dielectric susceptibility.

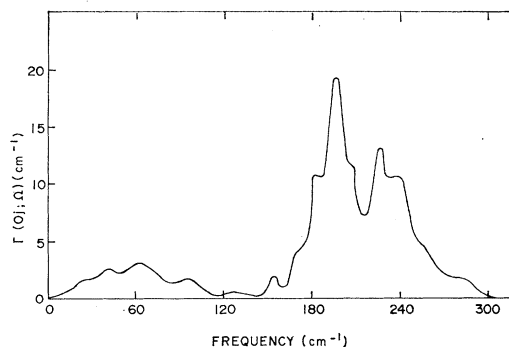


Fig. 7. Anti-Hermitian part of the  $\mathbf{k}=0$  self-energy matrix for KCl.

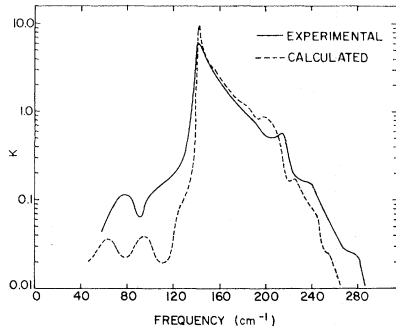


FIG. 8. Experimental and calculated extinction coefficient for KCl at  $T=300^\circ\text{K}$ .

The  $M_\alpha(0j)$  coefficient as it occurs in the numerator of Eq. (22) was evaluated by the expression<sup>21</sup>

$$\left(\frac{2\omega(0j)}{N\hbar}\right)^{1/2} M_\alpha(0j) = \sum_K \sum_\beta \frac{M_{\alpha,\beta}(K)}{M_K^{1/2}} m_\alpha(0j|K). \quad (25)$$

The symbols and summations appearing in this equation, except for  $M_{\alpha,\beta}(K)$ , have been defined earlier in this paper. Wallis *et al.*<sup>22</sup> have shown that for an ionic crystal of the NaCl structure, the tensor  $M_{\alpha,\beta}(K)$  is given by

$$M_{\alpha,\beta}(K) = \epsilon_K \delta_{\alpha\beta}, \quad (26)$$

where

$$\epsilon_K = e_K^* \left/ \left[ 1 - \frac{4\pi(\alpha_+ + \alpha_-)}{3v} \right] \right., \quad (27)$$

$e_K^*$  is the Szigeti effective charge of the  $K$ th ion in the unit cell,  $\alpha_+$  and  $\alpha_-$  are the ionic polarizibilities of the positive and negative ions, and  $v$  is the volume of the unit cell.  $e_K^*$  has the same magnitude for both ions in the unit cell. Using the values of  $|e_K^*|$ ,  $\alpha_+$ ,  $\alpha_-$ , and  $v$  as given by Karo and Hardy,<sup>4</sup> the value of  $\epsilon$  was found and it is tabulated in Table I. Equation (25) can be expanded to yield

$$\left(\frac{2\omega(0j)}{N\hbar}\right)^{1/2} M_x(0j) = \left( \frac{m_x(0j|0)}{M_0^{1/2}} - \frac{m_x(0j|1)}{M_1^{1/2}} \right) \epsilon, \quad (28)$$

and thus the value of  $M_x(0j)$  was evaluated as given in Table I. Ipatova *et al.*<sup>9</sup> have also shown that the high-frequency susceptibility  $\chi_\alpha^E$  is given by

$$\chi_\alpha^E = \frac{1}{4\pi} \left( \frac{3\epsilon}{|e^*|} - 3 \right) = 0.094 \quad \text{for KCl.} \quad (29)$$

The complex susceptibility was calculated from  $\Gamma$  and  $\Delta_3$  and the coefficients  $M_\alpha(0j)$  and  $\chi^E$ . The real and imaginary parts of the complex index of refraction

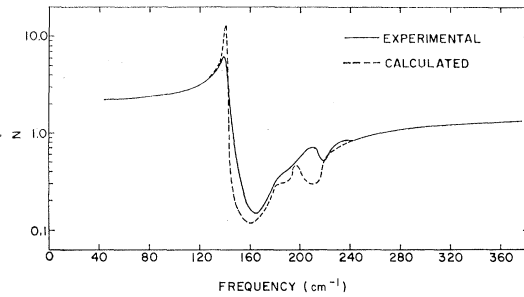


FIG. 9. Experimental and calculated index of refraction for KCl at  $T=300^\circ\text{K}$ .

$\hat{N}(\Omega) = N(\Omega) + iK(\Omega)$  were evaluated from the susceptibility and the results are given in Figs. 8 and 9.

#### IV. DISCUSSION

The qualitative agreement between the experimental and calculated values of the extinction coefficient appears to be very reasonable, especially on the high-frequency side of the fundamental absorption peak. From Fig. 8 it can be seen that there are three secondary maxima in the experimental data occurring at approximately 215, 240, and 275  $\text{cm}^{-1}$ . The spectral positions of these secondary maxima are somewhat higher than the calculated values which occur at 195, 225, and 250  $\text{cm}^{-1}$ , respectively. These discrepancies, we believe, can be traced to the values of the phonon frequencies used in the calculations because the calculated positions of the three sidebands correspond very closely to sum bands between the maxima in the KCl density-of-states curve. The density of states for the deformation-dipole model used by Karo and Hardy<sup>23</sup> shows three maxima occurring at approximately 85, 110, and 140  $\text{cm}^{-1}$ . The sum bands between any two of these frequencies are located at 195, 225, and 250  $\text{cm}^{-1}$ , which are where the three secondary maxima occur in the calculated extinction coefficient.

The largest discrepancies between the experimental and calculated values of the extinction coefficient occur at frequencies below the fundamental absorption peak, although the two curves appear to share some qualitative features. The shoulder and secondary maximum occurring in the experimental data at approximately 100 and 80  $\text{cm}^{-1}$ , respectively, seem to be reflected in the calculated curve which has a shoulder and maximum at approximately 130 and 100  $\text{cm}^{-1}$ . A second maximum in the calculated curve, occurring at 60  $\text{cm}^{-1}$ , does not appear in the experimental data. Below 130  $\text{cm}^{-1}$ , it is apparent from Fig. 8 that the quantitative agreement between the two curves is less satisfactory in both the spectral positions and magnitudes of the low-frequency sideband structure. As mentioned in Sec. II part of the discrepancies occurring in this region can be attributed to the inaccuracies in the experimental determination of

<sup>21</sup> Reference 5, p. 453, and Ref. 15, p. 305.

<sup>22</sup> R. F. Wallis and A. A. Maradudin, in *Proceedings of the International Conference on Physics of Semiconductors, Exeter, 1962* (The Institute of Physics and the Physical Society, London, 1962), p. 490.

<sup>23</sup> Reference 4, p. 2029.



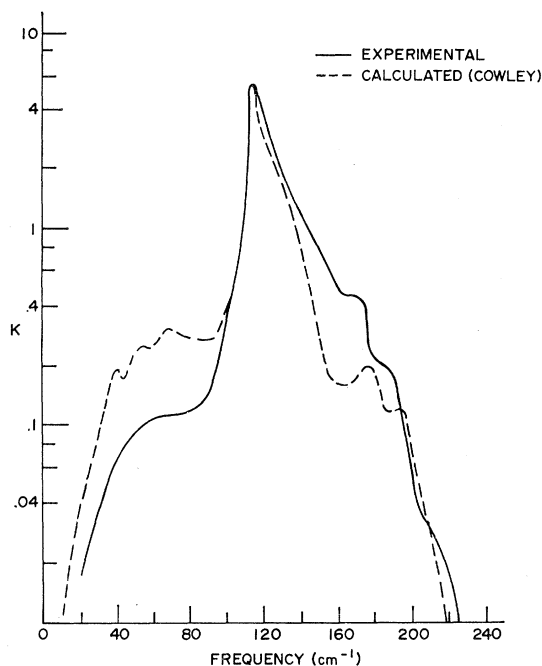


FIG. 10. Experimentally measured extinction coefficient of KBr at  $T=300^{\circ}\text{K}$  compared to the calculation made by Cowley. (See Ref. 5.)

$K(\Delta K/K \sim 0.3)$ . However, as evident from Fig. 8, this explanation is not sufficient in itself to account for the quantitative discrepancies below  $130\text{ cm}^{-1}$ , and we conclude that the calculated curve is too low. One possible explanation for this is that, because of computational difficulties, our calculation did not include three phonon processes which arise from the frequency-dependent quartic anharmonic contributions to  $\Gamma(0j; \Omega)$ . At elevated temperatures and at frequencies below the fundamental absorption peak these processes can be important.<sup>24</sup>

It is also possible that the asymmetry displayed in Fig. 8 between the calculated and experimental values of  $K$ , e.g., the calculated values are too small for  $\omega < \omega_{\text{TO}}$  and too large for  $\omega > \omega_{\text{TO}}$ , can be explained by the omission of the mixed one and two phonon processes which give rise to terms of this shape.<sup>25</sup>

The curves of the experimental and calculated values for the index of refraction are shown in Fig. 9. Again the two curves show some qualitative features in the spectral region between  $140$  and  $240\text{ cm}^{-1}$  where the index is less than unity.

Figures 10 and 11 show the comparisons between the experimental values of  $N$  and  $K$  for KBr obtained in this work and the numerical calculations of Cowley.<sup>5</sup> The calculations performed by Cowley on KBr are, in

<sup>24</sup> I. P. Ipatova, A. A. Maradudin, and R. F. Wallis, *Fiz. Tverd. Tela* **8**, 1064 (1966) [English transl.: *Soviet Phys.—Solid State* **8**, 850 (1966)]; *Phys. Rev.* **155**, 882 (1967).

<sup>25</sup> Terms of this type have been written by Cowley (see Ref. 5). In particular, the diagrams (c) and (d) in Fig. 10 in Cowley's paper give rise to the expression given by Eq. (6.10).

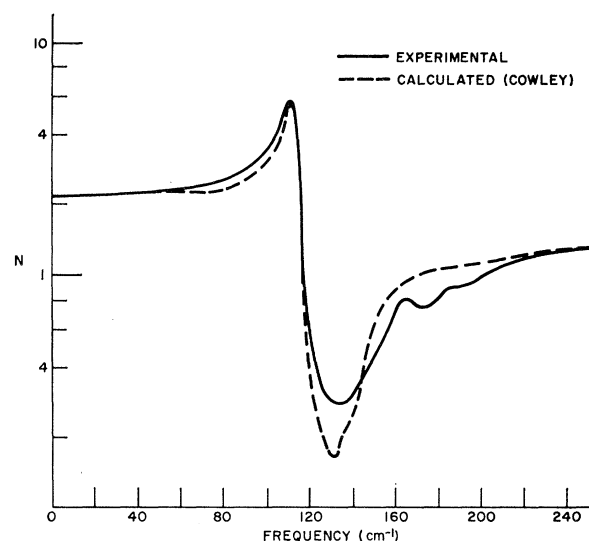


FIG. 11. Experimentally measured index of refraction of KBr at  $T=300^{\circ}\text{K}$ , compared to the calculation made by Cowley. (See Ref. 5.)

principle, more accurate than those presented in this paper for KCl because he included the contributions to the complex index of refraction arising from the second-order dipole moment (which were neglected in the present work), and his eigendata were derived from the dispersion curves of KBr as measured by neutron diffraction techniques.

## V. CONCLUSION

Asymmetric Fourier-transform spectroscopy is a very powerful technique for measuring the far-infrared properties of solids because both the real and imaginary parts of the complex amplitude reflectance (or transmittance) can be measured simultaneously. Two alkali halides, KCl and KBr, were measured in reflection to demonstrate the usefulness of this technique for studying the sideband structure caused by phonon interactions. The detailed numerical calculations of  $N$  and  $K$  performed on KCl in this paper and the results on KBr by Cowley<sup>5</sup> were shown to be in reasonable agreement with the experimental ones.

## ACKNOWLEDGMENTS

The authors wish to express their thanks to Dr. R. Sanderson, Dr. E. Russell, Dr. R. Gillespie, Dr. R. Ulrich, and Dr. J. Berg for their many discussions and assistance during the course of this work. We are also indebted to Professor L. Genzel for providing the initial impetus for this work and for his reading of the final manuscript. The Ohio State Numerical Computation Center is gratefully acknowledged for the granting of generous amounts of computer time. We also wish to thank the Bell Telephone Laboratories for helping in the preparation of the manuscript.